[^{64}Cu-NOTA-8-Aoc-BBN(7-14)NH_2] targeting vector for positron-emission tomography imaging of gastrin-releasing peptide receptor-expressing tissues

Adam F. Prasanphanich*†, Prasant K. Nanda*, Tammy L. Rold‡, Lixin Ma*†§, Michael R. Lewis†¶, Jered C. Garrison†‡, Timothy J. Hoffman†‡, Gary L. Sieckman†, Said D. Figueroa*†, and Charles J. Smith*†‖**

Departments of *Radiology and ‡Internal Medicine, and §International Institute of Nano and Molecular Medicine, University of Missouri School of Medicine, Columbia, MO 65211; †Research Division, Harry S. Truman Memorial Veterans' Hospital, Columbia, MO 65201; ‖University of Missouri Research Reactor, University of Missouri, Columbia, MO 65211; and ¶Department of Veterinary Medicine and Surgery, University of Missouri College of Veterinary Medicine, Columbia, MO 65211

Communicated by M. Frederick Hawthorne, University of Missouri, Columbia, MO, June 11, 2007 (received for review March 29, 2007)

Radiolabeled peptides hold promise as diagnostic/therapeutic targeting vectors for specific human cancers. We report the design and development of a targeting vector, [^{64}Cu-NOTA-8-Aoc-BBN(7-14)NH_2] (NOTA = 1,4,7-triazacyclononane-1,4,7-triacetic acid, 8-Aoc = 8-aminooctanoic acid, and BBN = bombesin), having very high selectivity and affinity for the gastrin-releasing peptide receptor (GRPr). GRPrs are expressed on a variety of human cancers, including breast, lung, pancreatic, and prostate, making this a viable approach toward site-directed localization or therapy of these human diseases. In this study, [NOTA-X-BBN(7-14)NH_2] conjugates were synthesized, where X = a specific pharmacokinetic modifier. The IC_{50} of [NOTA-8-Aoc-BBN(7-14)NH_2] was determined by a competitive displacement cell-binding assay in PC-3 human prostate cancer cells using ^{125}I-[Tyr^4]-BBN as the displacement ligand. An IC_{50} of 3.1 ± 0.5 nM was obtained, demonstrating high binding affinity of [NOTA-8-Aoc-BBN] for the GRPr. [^{64}Cu-NOTA-X-BBN] conjugates were prepared by the reaction of $^{64}CuCl_2$ with peptides in buffered aqueous solution. *In vivo* studies of [^{64}Cu-NOTA-8-Aoc-BBN(7-14)NH_2] in tumor-bearing PC-3 mouse models indicated very high affinity of conjugate for the GRPr. Uptake of conjugate in tumor was 3.58 ± 0.70% injected dose (ID) per g at 1 h postintravenous injection (p.i.). Minimal accumulation of radioactivity in liver tissue (1.58 ± 0.40% ID per g, 1 h p.i.) is indicative of rapid renal-urinary excretion and suggests very high *in vivo* kinetic stability of [^{64}Cu-NOTA-8-Aoc-BBN(7-14)NH_2] with little or no *in vivo* dissociation of $^{64}Cu^{2+}$ from the NOTA chelator. Kidney accumulation at 1 h p.i. was 3.79 ± 1.09% ID per g. Molecular imaging studies in GRPr-expressing tumor models produced high-contrast, high-quality micro-positron-emission tomography images.

bombesin | copper 64 | molecular imaging | PC-3 tumors

In recent years, nuclear medicine researchers have been investigating the potential of radiolabeled peptides to target selective receptors expressed on human tumor cancer cells (1–10). Successful targeting of somatostatin receptor-positive tumors by receptor-specific diagnostic radiopharmaceuticals has pioneered efforts by others to develop new biologically active targeting vectors that have high affinity and selectivity for human tumors (1, 2, 11). Bombesin (BBN) peptide, an amphibian homologue of mammalian gastrin-releasing peptide (GRP), has demonstrated the ability to bind with high affinity and specificity to the GRP receptor (GRPr) (12, 13). GRPrs are expressed on a variety of human cancers including breast, lung, and pancreatic cancers (12, 13). High-affinity GRPr expression has also been identified in tissue biopsy samples of human prostate cancer (14–16). Markwalder and Reubi (14) demonstrated that GRPr expression in primary prostatic invasive carcinoma was present in 100% of the tissues tested, and in 83% of these cases GRPr expression was determined to be high or very high (1,000 dpm/mg tissue). Prostate cancer is the most commonly diagnosed and a leading cause of cancer death in men in the United States. An estimated 218,890 new cases of prostate cancer will be reported in 2007, resulting in 27,050 deaths (17). Failure of current therapies to prolong patient survival provides some impetus to develop new and innovative diagnostic and treatment strategies for patients with prostate cancer (18–20), making radiolabeled, site-directed targeting vectors based on peptides a viable approach toward diagnosis or therapy of this human disease.

Copper-64 radionuclide continues to be investigated as a promising isotope for site-directed positron-emission tomography (PET) and radiotherapy (21). Receptor-specific peptide conjugates containing the chelating agents DOTA (1,4,7,10-tetraazacyclododecane-1,4,7,10-tetraacetic acid) and TETA (1,4,8,11-tetraazacyclotetradecane-1,4,8,11-tetraacetic acid) have shown some promise for production of Cu-64-labeled targeting vectors (22–26). However, $^{64}Cu^{2+}$ complexes of these specific chelating ligands are only moderately stable under *in vivo* conditions, resulting in demetallation and subsequent accumulation in nontarget tissues such as liver. Cross-bridged, cyclam-based ligand frameworks appended to specific biologically active targeting vectors offer improved kinetic stability to *in vivo* transmetallation reactions with various proteins in comparison with DOTA and TETA (27–29). However, ligands of this general type still suffer from difficult synthetic protocols and renal accumulation and retention of ^{64}Cu radionuclide (27–29). Thus, there is some impetus to improve the *in vivo* kinetic stability of ^{64}Cu-macrocyclic bioconjugates to reduce accumulation in collateral tissues such as liver (22–26). Furthermore, reduction of uptake in normal kidney would do much to improve the inherent renal toxicities of many peptide-based therapeutic agents (27–29). Previous studies have described the potential use of NOTA (1,4,7-triazacyclononane-1,4,7-triacetic acid) as a bifunctional chelating agent for divalent copper (30, 31). NOTA has the capacity to form stable complexes with Cu^{2+} and a host of other divalent and trivalent metal centers (32, 33) and therefore may help to produce conjugates that overcome demetallation and uptake of tracer in hepatic tissue. The overall

Author contributions: A.F.P. and C.J.S. designed research; A.F.P., P.K.N., T.L.R., L.M., G.L.S., and S.D.F. performed research; A.F.P., P.K.N., T.J.H., and C.J.S. contributed new reagents/analytic tools; A.F.P., P.K.N., T.L.R., L.M., M.R.L., J.C.G., T.J.H., G.L.S., S.D.F., and C.J.S. analyzed data; and A.F.P., L.M., M.R.L., T.J.H., S.D.F., and C.J.S. wrote the paper.

The authors declare no conflict of interest.

Freely available online through the PNAS open access option.

Abbreviations: BBN, bombesin; GRP, gastrin-releasing peptide; GRPr, GRP receptor; NOTA, 1,4,7-triazacyclononane-1,4,7-triacetic acid; DOTA, 1,4,7,10-tetraazacyclododecane-1,4,7,10-tetraacetic acid; TETA 1,4,8,11-tetraazacyclotetradecane-1,4,8,11-tetraacetic acid; PET, positron-emission tomography; p.i., postintravenous injection; FDG, 2-[^{18}F]fluoro-2-deoxy-D-glucose; ID, injected dose; CT, computed tomography.

**To whom correspondence should be addressed. E-mail: smithcj@health.missouri.edu.

www.pnas.org/cgi/doi/10.1073/pnas.0705347104

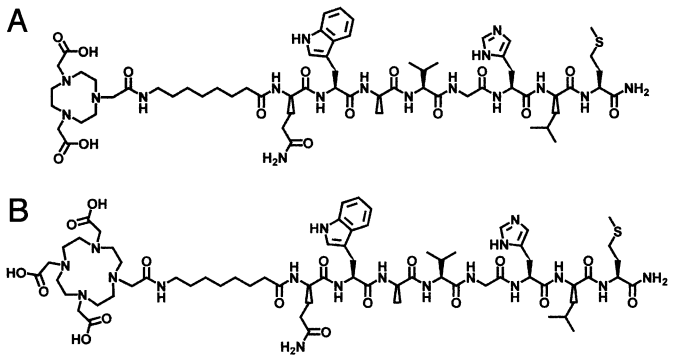

Fig. 1. Chemical structures of [NOTA-8-Aoc-BBN(7-14)NH_2] (*A*) and [DOTA-8-Aoc-BBN(7-14)NH_2] (*B*) conjugates.

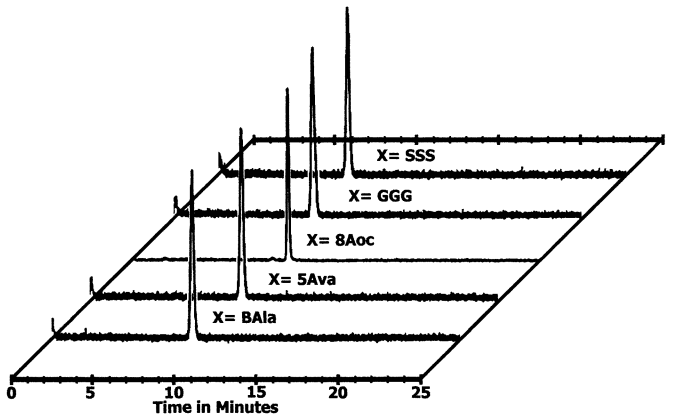

Fig. 2. RP-HPLC chromatographic profiles of purified [^{64}Cu-NOTA-X-BBN(7-14)NH_2] conjugates. BAl, β-alanine; 5Ava, 5-aminovaleric acid; 8Aoc, 8-aminooctanoic acid; GGG, glycylglycylglycine; SSS, serylserylserine.

neutral charge of the Cu^{2+}–NOTA conjugate may do much to improve accumulation and retention of conjugate in normal kidney tissue as well.

In the current study, we report the synthesis of a series of NOTA–BBN targeting vectors having very high affinity and selectivity for the GRPr. This article describes, in detail, synthesis and characterization of conjugates, radiometallation studies to produce [^{64}Cu-NOTA-X-BBN(7-14)NH_2]-conjugates, and detailed *in vitro* and *in vivo* investigations of [NOTA-8-Aoc-BBN(7-14)NH_2] (Fig. 1) and [^{64}Cu-NOTA-8-Aoc-BBN(7-14)NH_2] in a human, prostate, PC-3 tumor model. Previous studies in our laboratories and others (23, 34, 35) have indicated radiolabeled [DOTA-8-Aoc-BBN(7-14)NH_2] (Fig. 1) satisfies inherent *in vitro* and *in vivo* requirements for radiopharmaceutical development, including binding affinity, biodistribution, and GRPr-targeting ability. We have therefore based the current studies for [^{64}Cu-NOTA-8-Aoc-BBN(7-14)NH_2] on these previous models for direct comparison. *In vivo* microPET/microcomputed tomography (CT) studies in rodents bearing human, PC-3, xenografted prostate tumors administered with [^{64}Cu-NOTA-8-Aoc-BBN(7-14)NH_2] are also presented herein.

Results

All of the nonmetallated BBN conjugates used in this study were purified by RP-HPLC and characterized by electrospray ionization-MS (Table 1). NOTA-BBN targeting vectors were metallated with ^{64}Cu radionuclide in very high yield by addition of $^{64}CuCl_2$ to free conjugate in buffered, aqueous solution. For example, radiolabeling yields were ≥90% for all of the new peptide conjugates. All of the radiolabeled peptides that were used in this study were purified by RP-HPLC to produce conjugates of very high radiochemical purity and specific activity. Reversed-phase chromatograms of the new conjugates are demonstrated in Fig. 2. Each of the five chromatograms show a single species with retention times of 8.3, 9.0, 9.2, 8.2, and 7.6 min for pharmacokinetic modifiers X = β-Ala (β-alanine), 5-Ava (5-aminovaleric acid), 8-Aoc (8-aminooctanoic acid), GGG (glycylglycylglycine), and SSS (serylserylserine), respectively. Retention times for the native unlabeled peptides are 9.1, 9.3, 9.9, 8.7, and 8.1 min for X = β-Ala, 5-Ava, 8-Aoc, GGG, and SSS, respectively, demonstrating the effectiveness of the HPLC separation procedure to produce high specific activity products (Table 1). These conjugates demonstrated *in vitro* stability (RP-HPLC) for periods in excess of 18 h.

To assess the binding affinity of [NOTA-8-Aoc-BBN(7-14)NH_2] for the GRPr, competitive binding displacement assays in human prostate PC-3 tumor cells were performed where ^{125}I-[Tyr^4]-BBN was used as the displacement radioligand. These studies demonstrated competitive binding affinity of [NOTA-8-Aoc-BBN(7-14)NH_2] for the GRPr with an IC_{50} of 3.1 ± 0.5 nM.

In vivo studies of [^{64}Cu-NOTA-8-Aoc-BBN(7-14)NH_2] in normal CF-1 mice (n = 5) demonstrated effective clearance of conjugate from the bloodstream [i.e., 0.29 ± 0.10% injected dose (ID) per g in whole blood at 1 h postintravenous injection (p.i.)] and was excreted primarily via the renal-urinary excretion pathway with ≈76% of the ID being eliminated from the body at 4 h p.i. [^{64}Cu-NOTA-8-Aoc-BBN(7-14)NH_2] showed receptor-mediated uptake in normal pancreatic tissue, an organ known to express the GRPr in very high numbers in rodents (34–36). In human pancreatic tissue, however, the GRPr is expressed only minimally (12), and therefore limits the likelihood of radiotoxicity to normal pancreas of human patients using conjugates of this general type. In this study, uptake of [^{64}Cu-NOTA-8-Aoc-BBN] in normal pancreas was 27.0 ± 3.18% ID per g at 1 h p.i. Retention of radioactivity in pancreas is minimal at 24 h p.i., with only 1.42 ± 0.13% ID per g remaining in normal tissue. Furthermore, there appears to be little or no *in vivo* dissociation of $^{64}Cu^{2+}$ from the NOTA chelator as evident by absence of liver accumulation of radioactivity at 1 h p.i. (i.e., uptake in liver at 1 h p.i. was found to be 1.54 ± 0.59% ID per g). Kidney accumulation at 1 h p.i. was 2.92 ± 0.64% ID per g.

Detailed *in vivo* studies of [^{64}Cu-NOTA-8-Aoc-BBN(7-14)NH_2] in SCID mice bearing human PC-3 tumor xenografts showed receptor-mediated accumulation of 3.59 ± 0.70% ID per g in tumor tissue at 1 h p.i. (Fig. 3). Retention of [^{64}Cu-NOTA-

Table 1. Characterization of NOTA-BBN conjugates

Spacer, X	β-Ala	5-Ava	8-Aoc	GGG	SSS
Calculated molecular mass, kDa	1,297.5	1,325.7	1,367.6	1,397.6	1,487.7
Electrospray ionization molecular mass, kDA	1,297.9	1,325.6	1,367.6	1,397.6	1,487.8
Formula	$C_{58}H_{89}N_{17}O_{15}S$	$C_{60}H_{93}N_{17}O_{15}S$	$C_{63}H_{99}N_{17}O_{15}S$	$C_{61}H_{93}N_{19}O_{17}S$	$C_{64}H_{99}N_{19}O_{20}S$
HPLC t_R, min	9.1	9.3	9.9	8.7	8.1
HPLC t_R (^{64}Cu), min	8.3	9.0	9.2	8.2	7.6

β-Ala, β-alanine; 5-Ava, 5-aminovaleric acid; 8-Aoc, 8-aminooctanoic acid; GGG, glycylglycylglycine; SSS, serylserylserine.

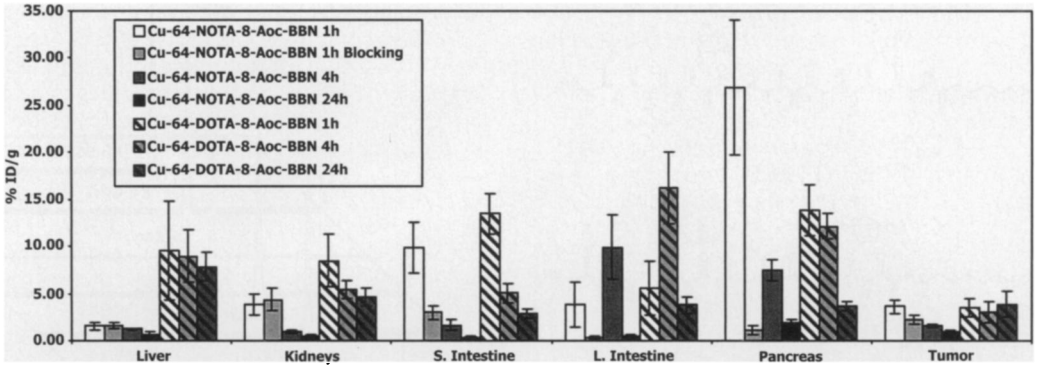

Fig. 3. Pharmacokinetic data for [^{64}Cu-NOTA-8-Aoc-BBN(7-14)NH_2] and [^{64}Cu-DOTA-8-Aoc-BBN(7-14)NH_2] in PC-3 tumor-bearing mice as percent ID per g at 1-, 4-, and 24-h time points.

8-Aoc-BBN(7-14)NH_2] in tumor tissue was evident at 24 h p.i. For example, 1.00 ± 0.19% ID per g remained in whole tumor at 24 h p.i., demonstrating internalization behavior and subsequent intracellular trapping mechanisms for agonist ligands of this general type (36). Blocking studies, in which 100 μg of commercially available BBN[1-14] was administered 15 min before [^{64}Cu-NOTA-8-Aoc-BBN(7-14)NH_2], reduced accumulation of radioactivity in tumor tissue at 1 h p.i. to 2.22 ± 0.52% ID per g, further demonstrating the ability of [^{64}Cu-NOTA-8-Aoc-BBN(7-14)NH_2] to target GRPr with very high specificity and affinity. Addition of blocking agent reduced receptor-mediated pancreatic uptake by ≈95%. Intestinal accumulation was reduced by ≈75%, suggesting some of the uptake in the intestinal tract to be receptor mediated and not purely driven by hepatobiliary excretion. Maina *et al.* (37) have reported similar findings.

MicroPET imaging studies of [^{64}Cu-NOTA-8-Aoc-BBN(7-14)NH_2] in PC-3 tumor-bearing mice at 24 h p.i. demonstrated the utility of this conjugate to be potentially used as a site-directed PET targeting agent for primary or metastatic prostate cancer. Briefly, 1.5 mCi of [^{64}Cu-NOTA-8-Aoc-BBN(7-14)NH_2] was administered to the rodent and subsequent imaging studies were performed. Fig. 4 shows maximum-intensity microPET images with uptake and retention of conjugate in tumor and minimal accumulation of radioactivity in collateral tissues, making diagnostic PET imaging of prostate tumors of the lower abdomen with [^{64}Cu-NOTA-8-Aoc-BBN(7-14)NH_2] possible. Some accumulation and retention of radioactivity is observed in liver and correlates well with biodistribution data and a tumor/liver ratio of ≈1.4 at 24 h p.i.

Discussion

Pancreatic tissue in rodents is the only accessible organ that expresses the GRPr in very high numbers (34–36). Therefore, accumulation of [^{64}Cu-NOTA-8-Aoc-BBN(7-14)NH_2] in normal CF-1 rodent models was indicative of a high-affinity radioligand for the GRPr and necessitated *in vivo* biodistribution studies in rodents bearing human PC-3 tumor xenografts. Accumulation and retention of [^{64}Cu-NOTA-8-Aoc-BBN(7-14)NH_2] in SCID mice bearing PC-3 tumors is comparable with uptake of ^{64}Cu-DOTA-Aoc-BBN(7-14) conjugate in PC-3-bearing athymic mice recently reported by Rogers *et al.* (23). Rogers *et al.* report 5.5 ± 0.6% ID per g in tumors at 1 h p.i. with significant retention even at 24 h (i.e., t = 24 h p.i.; 2.5 ± 0.5% ID per g) (23). High tumor uptake at 24 h p.i. for this conjugate is a direct result of demetallation of $^{64}Cu^{2+}$ from the DOTA-chelating ligand and subsequent intertumoral trapping of radionuclide. Chen and coworkers (24, 25) have reported synthesis and radiolabeling investigations of DOTA-[Lys^3]-BBN with ^{64}Cu radionuclide to produce ^{64}Cu-DOTA-[Lys^3]-BBN conjugate. In those studies, they show uptake and accumulation data of 3.97 ± 0.15% ID per g in PC-3 tumor at 1 h p.i. For each of the two conjugates ^{64}Cu-DOTA-Aoc-BBN(7-14) (23) and ^{64}Cu-DOTA-[Lys^3]-BBN (24, 25), accumulation and retention in normal liver was evident. ^{64}Cu-DOTA-[Lys^3]-BBN uptake in liver tissue was 4.18 ± 0.63% ID per g at 1 h p.i (24, 25). ^{64}Cu-DOTA-Aoc-BBN(7-14) conjugate showed very high uptake and retention of radioactivity in liver tissue with ≈10% and 5% ID per g at 1 and 24 h p.i., respectively (23). Anderson *et al.* (26) have observed similar results in liver tissue for ^{64}Cu-TETA-octreotide, an agent that has shown significant promise toward inhibiting the growth of somatostatin, receptor-positive tumors. High accumulation of these conjugates in liver is potentially caused by dissociation of ^{64}Cu radionuclide from the DOTA or TETA chelators *in vivo* and subsequent coordination to superoxide dismutase in liver tissue (26). Accumulation of [^{64}Cu-NOTA-8-Aoc-BBN(7-14)NH_2] in liver tissue was considerably lower than ^{64}Cu-based peptide conjugates ^{64}Cu-DOTA-Aoc-BBN(7-14) (23) and ^{64}Cu-DOTA-[Lys-3]-BBN (24, 25). For example, only 1.54 ± 0.49% ID per g of conjugate accumulated in liver of normal mice at 1 h p.i. Reduced

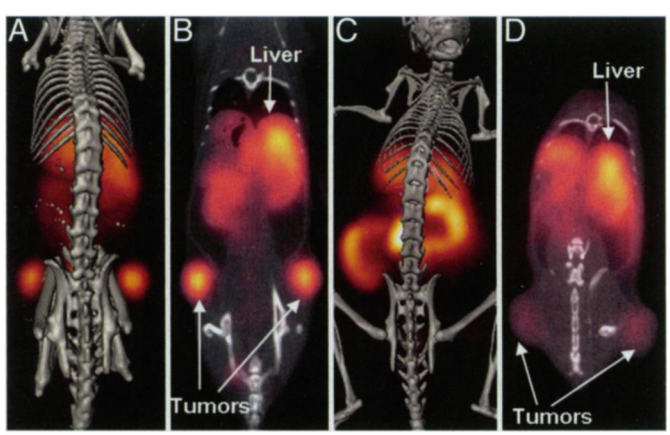

Fig. 4. *In vivo* microPET/CT and microMRI images of a PC-3 tumor-bearing mouse 24 h after tail vein injection of [^{64}Cu-NOTA-8-Aoc-BBN(7-14)NH_2] or [^{64}Cu-DOTA-8-Aoc-BBN(7-14)NH_2] (liver and bilateral, xenografted left and right flank tumors are denoted by white arrows). (*A*) Maximum intensity microPET tumor and microCT skeletal fusion coronal image for [^{64}Cu-NOTA-8-Aoc-BBN(7-14)NH_2]. (*B*) MicroPET coronal image slice showing specific tumor uptake of [^{64}Cu-NOTA-8-Aoc-BBN(7-14)NH_2]. (*C*) Maximum intensity microPET tumor and microCT skeletal fusion coronal image for [^{64}Cu-DOTA-8-Aoc-BBN(7-14)NH_2]. (*D*) MicroPET coronal image slice showing specific tumor uptake of [^{64}Cu-DOTA-8-Aoc-BBN(7-14)NH_2].

accumulation of [^{64}Cu-NOTA-8-Aoc-BBN(7-14)NH_2] in liver tissue could be merely a consequence of rapid renal-urinary excretion. Kukis *et al.* (31) have reported on the stability of ^{67}Cu-radiolabeled 6-[*p*-(bromoacetamido)benzyl]-TETA-, 2-[*p*-(bromoacetamido)benzyl]-TETA-, 2-[*p*-(bromoacetamido)benzyl]-NOTA-, and 2-[*p*-(bromoacetamido)benzyl]-DOTA-murine antilymphoma IgG_{2a} (Lym-1 immunoconjugate) conjugates in human serum. In that study, they show rate of loss of Cu-67 from conjugate to be ≈1% per day for all conjugates other than 2-[*p*-(bromoacetamido)benzyl]-TETA-Lym-1, which showed ≈4% loss of ^{67}Cu radionuclide from immunoconjugate. It is not clearly understood whether reversible, noncovalent interactions in the immunoconjugate have any influence on the kinetic stability of the metal–chelate complex in these conjugates. Small peptide conjugates of Cu(II) using DOTA- and TETA-chelating ligands, on the other hand, often suffer from demetallation and subsequent trapping of radionuclide in specific tissue. In this study, lack of retention of radioactivity in collateral tissues such as liver at later time points suggests a high degree of *in vivo* stability for [^{64}Cu-NOTA-8-Aoc-BBN(7-14)NH_2] as compared with peptide conjugates comprised of similar polyaminocarboxylate chelators such as DOTA and TETA (22–26). For *ex vivo* molecular imaging procedures such as PET, it is essential to have accumulation and prolonged retention of [^{64}Cu-NOTA-8-Aoc-BBN(7-14)NH_2] in GRPr-expressing tumor and lack of retention in collateral tissue to produce higher target-to-nontarget ratios and high-quality images. Kidney uptake and retention of [^{64}Cu-NOTA-8-Aoc-BBN(7-14)NH_2], as reported herein, was also demonstrably lower than the GRPr-specific conjugates ^{64}Cu-DOTA-Aoc-BBN(7-14) (23) and ^{64}Cu-DOTA-[Lys^3]-BBN (24, 25).

The results presented herein are not a direct comparison of pharmacokinetic properties of [^{64}Cu-NOTA-8-Aoc-BBN(7-14)NH_2] with ^{64}Cu-DOTA-Aoc-BBN(7-14) (23) and ^{64}Cu-DOTA-[Lys-3]-BBN (24, 25) because of differences in animal models, specific conjugate, or sampling times. Recent reports by Garrison *et al.* (38), however, do offer some insight into the *in vivo* effectiveness of [^{64}Cu-NOTA-8-Aoc-BBN(7-14)NH_2] as compared with Rogers *et al.*'s ^{64}Cu-DOTA-Aoc-BBN(7-14) conjugate in a direct comparative study. They have reported the synthesis of [^{64}Cu-DOTA-8-Aoc-BBN(7-14)NH_2] and subsequent animal studies in PC-3 tumor-bearing SCID mouse models (38). [^{64}Cu-DOTA-8-Aoc-BBN(7-14)NH_2] conjugate showed very high uptake and retention of radioactivity in liver tissue with 9.56 ± 5.20%, 6.95 ± 4.71%, and 7.80 ± 1.51% ID per g at 1, 4, and 24 h p.i., respectively (38). Uptake in tumor tissue at 1 h p.i. was 3.48 ± 0.90% ID per g. Retention of radioactivity in tumor at 24 h p.i. (3.88 ± 1.40% ID per g; Fig. 3) indicated demetallation and trapping of $^{64}Cu^{2+}$ in tumor tissue, similar to reports presented by Rogers *et al.* (23) in tumor-bearing athymic mice. MicroPET imaging studies at 24 h p.i. (Fig. 4) for [^{64}Cu-DOTA-8-Aoc-BBN(7-14)NH_2] in PC-3 tumor-bearing mice were unremarkable in tumor tissue, with significant collateral abdominal accumulation presumably caused by free ^{64}Cu radionuclide (38).

In this study, we have demonstrated the effectiveness of using NOTA chelator to produce a kinetically inert BBN conjugate having very high affinity for GRPrs overexpressed on PC-3 prostate cancer cells. Recently, investigators have begun to overcome many of the inherent difficulties of DOTA and TETA chelators for producing *in vivo* stable conjugates with ^{64}Cu radionuclide by introduction of a new class of cross-bridged chelating ligand framework for this radiometal (27–29). These new chelators have shown marked promise to be used as integral components of site-directed targeting vectors based on octreotide (27). However, targeting vectors of this specific type suffer from retention in normal kidney, presumably because of the overall +1 charge of the conjugate (27). This could limit the utility of these conjugates to be used for PET imaging of neuroendocrine tumors of the abdomen. Furthermore, renal toxicity continues to be a major drawback for therapy-based peptide conjugates using β-emitting radionuclides and may limit the therapeutic efficacy of ^{64}Cu/^{67}Cu-conjugates (27–29) of this general type. In the current study, uptake of [^{64}Cu-NOTA-8-Aoc-BBN(7-14)NH_2] in normal kidney was very similar to ^{64}Cu-CB-TE2A-Y3-TATE at 1 h p.i. [^{64}Cu-NOTA-8-Aoc-BBN(7-14)NH_2], however, uses dianionic NOTA chelator to stabilize the +2 charge on the metal center, producing neutral peptide conjugates that may overcome prolonged retention in renal tissue, even at 24 h p.i. For example, only 0.42 ± 0.04% ID per g of [^{64}Cu-NOTA-8-Aoc-BBN(7-14)NH_2] remained in normal kidney at 24 h p.i. Therefore, conjugation of NOTA chelator to somatostatin receptor subtype 2 targeting vectors offers an alternative approach for producing kinetically inert ^{64}Cu conjugates having reduced renal retention for imaging and possible treatment of neuroendocrine tumors.

[^{64}Cu-NOTA-8-Aoc-BBN(7-14)NH_2] offers considerable promise for molecular imaging and potential therapy of prostate cancer in human patients. By 2005 the use of 2-[^{18}F]fluoro-2-deoxy-D-glucose (FDG) in PET had become a clinical imaging standard for diagnosis, staging, and restaging of 10 types of cancer (39). However, there is mounting evidence that FDG-PET is not useful for imaging most presentations of prostate cancer. Major limitations of FDG-PET in the diagnosis of prostate cancer include low uptake in primary tumors and excretion of FDG in the urine (40). Furthermore, FDG-PET cannot distinguish prostate carcinoma from benign prostatic hyperplasia, postoperative scar tissue, or local recurrence after radical prostatectomy (41). It has been suggested that FDG-PET may play a role in staging lymph node and skeletal metastases (40). However, Sung *et al.* (42) found that FDG-PET was not useful for patients with metastatic disease undergoing treatment or who have undetectable prostate-specific antigen (PSA) levels. They determined that staging of advanced prostate cancer using FDG-PET was useful only for patients who either had been untreated, had an incomplete therapeutic response, or had presented with rising PSA levels during or after therapy. The only prostate cancer imaging agent approved by the U.S. Food and Drug Administration is the radiolabeled antibody ^{111}In-DTPA-7E11-C5.3 (ProstaScint). The use of ProstaScint for imaging prostate cancer remains controversial (43), because the antibody binds an intracellular epitope of prostate-specific membrane antigen and only necrotic tumor cells can be detected. On the basis of these results, more accurate, sensitive, and specific noninvasive tests for all stages of prostate cancer are clearly warranted. [^{64}Cu-NOTA-8-Aoc-BBN(7-14)NH_2] has considerable potential to overcome the limitations of FDG and ProstaScint for diagnosis, staging, and restaging of this disease by targeting GRPrs up-regulated in locally confined, invasive, and metastatic prostate cancer.

In summary, the data presented herein suggest that [^{64}Cu-NOTA-8-Aoc-BBN(7-14)NH_2] may present higher resistance to transmetallation reactions *in vivo* as compared with other larger polyaminocarboxylate chelators. Studies show that the size of the parent macrocycle has a significant effect on the *in vivo* stability of ^{64}Cu conjugates (28). The more compact, neutral ^{64}Cu-NOTA complex of [^{64}Cu-NOTA-8-Aoc-BBN(7-14)NH_2] appears to overcome demetallation and uptake of tracer by hepatobiliary proteins and accumulation and retention of conjugate in renal tissue *in vivo*, producing microPET images that are clearly superior to other conjugates described herein (23–29). Furthermore, ease of ligand synthesis, conjugation protocols, and radiolabeling techniques satisfies nearly all of the inherent require-

ments for production of site-directed radiopharmaceuticals of this type.

Materials and Methods

RP-HPLC. Purified peptides and radiolabeled conjugates were prepared by using a SCL-10A HPLC system (Shimadzu, Kyoto, Japan) equipped with an in-line SPD-10A UV-visible absorption detector (Shimadzu) (λ = 280 nm) and an in-line ORTEC NaI solid crystal scintillation detector (EG & G, Salem, MA). EZStart software (7.3) (Shimadzu) was used for data acquisition of both signals. A reversed-phase column (Jupiter 4μ Proteo; 90 Å, 250 × 4.6 mm; Phenomenex, Belmont, CA) was used at a constant temperature setting of 34°C (CH-30 column heater; Eppendorf, Hamburg, Germany). HPLC-grade acetonitrile was purchased from Fisher Scientific (Waltham, MA). The mobile phase consisted of a linear gradient system at a flow rate of 1.5 ml/min: solvent A, 100% water with 0.1% trifluoroacetic acid (TFA); solvent B, 100% acetonitrile with 0.1% TFA. Purification of the unligated peptide took place by using a linear gradient of 95:5 A/B to 20:80 A/B over 25 min, followed by an additional 5 min at 20:80 A/B. Purification and labeling of all NOTA-conjugated peptides took place by using a linear gradient of 25:75 A/B to 35:65 A/B gradient over 15 min, followed by an additional 10 min at 5:95 A/B. Purified peptides conjugates were lyophilized on a CentriVap system (Labconco, Kansas City, MO).

Solid-Phase Peptide Synthesis of BBN Conjugates. Conventional Fmoc protection solid-phase peptide synthesis was used to synthesize the unligated [H_2N-X-BBN(7-14)NH_2] peptides as described (36). Crude peptides were purified by RP-HPLC and characterized by electrospray ionization-MS.

Synthesis of [NOTA-X-BBN(7-14)NH_2] Peptides. Manual conjugation of the NOTA bifunctional chelating agent to purified [H_2N-X-BBN(7-14)NH_2] peptides took place in buffered aqueous solution with coupling reagents purchased from Pierce Biotechnology (Rockford, IL). NOTA was prepared as described (33). The initial buffered solution consisted of 0.1 M 2-[morpholino] ethanesulfonic acid at pH 4.7 (Mes). Three milligrams of [H_2N-X-BBN(7-14)NH_2] (1 molar equivalent) was dissolved in 200 μl of 0.1 M sodium phosphate buffer at pH 7.0 (solution 1). Similarly, 50 equivalents of sulfo-*N*-hydroxysulfosuccinimide was dissolved in 100 μl of Mes (solution 2). Fifty equivalents of NOTA were dissolved in 0.5 ml of Mes, and the pH was adjusted to pH 4.7 by addition of 10% NaOH solution (solution 3). Before addition of NOTA to [H_2N-X-BBN(7-14)NH_2], 15 equivalents of 1-ethyl-3-(dimethylaminopropyl)carbodiimide was dissolved in 100 μl of Mes at pH 7.0 (solution 4). Together at room temperature, solutions 2–4 were allowed to stir for 10 min at pH 4.7. Solution 1 was added to this mixture, and the pH was carefully adjusted to 7.0 with 10% NaOH. The reaction was allowed to run overnight after which conjugates were purified and characterized as described.

***In Vitro* Cell Binding Affinity Studies.** A competitive displacement binding assay was used to determine the affinity for [NOTA-8-Aoc-BBN(7-14)NH_2] using ^{125}I-[Tyr^4]-BBN (Perkin–Elmer, Waltham, MA) as the displacement radioligand. Approximately 3×10^6 PC-3 cells were incubated with 20,000 cpm of ^{125}I-[Tyr^4]-BBN and known increasing concentrations of [NOTA-8-Aoc-BBN(7-14)NH_2] at 37°C for 1 h. Cell media, DMEM/F-12K, consisted of 0.01 M MEM and 2% BSA, pH 5.5. The medium was aspirated and washed four times after incubation. Cell-associated radioactivity was then determined by counting the washed cells in a Riastar multiwell gamma counting system (Packard) and the IC_{50} was calculated.

Synthesis of the [^{64}Cu-NOTA-X-BBN] Conjugates. [NOTA-X-BBN(7-14)NH_2] conjugates (100 μg) were dissolved in 200 μl of 0.4 M ammonium acetate at pH 7.0. To this was added 50 μl of $^{64}CuCl_2$, pH < 3. The pH of the resultant solution was 6.5. The solution was heated for 1 h at 70°C. Radiolabeled conjugates were purified by RP-HPLC and collected into 100 μl of 1 μg/μl aqueous BSA. A stream of N_2 was used to evaporate aceotnitrile followed by quality control via an analytical radiometric chromatographic profile to determine radiochemical purity and stability.

Pharmacokinetic Studies in Normal Mice. All animal studies were conducted in accordance with the highest standards of care as outlined in the National Institutes of Health Guide for Care and Use of Laboratory Animals and the Policy and Procedures for Animal Research at the Harry S. Truman Memorial Veterans' Hospital. The biodistribution studies of [^{64}Cu-NOTA-8-Aoc-BBN(7-14)NH_2] were determined in normal (CF-1) mice. The mice were injected with 7 μCi of the ^{64}Cu conjugate in 100 μl of isotonic saline via the tail vein. The mice were killed, and tissues and organs were excised from the animals at 1, 4, and 24 h p.i. Subsequently, the tissues and organs were weighed and counted in a NaI well counter, and the percent ID and percent ID per g of each organ or tissue were calculated. The percent ID in whole blood was estimated assuming a whole-blood volume of 6.5% the total body weight. Urine was estimated and reported as percent ID and consisted of urine, bladder, and cage paper radioactivity.

Pharmacokinetic Studies in Mice Bearing Human Prostate Tumors. SCID mice bearing xenografted human PC-3 tumors were used to determine the ability of [^{64}Cu-NOTA-8-Aoc-BBN(7-14)NH_2] to target tumor *in vivo*. For studies involving tumor-bearing mice, 4- to 5-week-old female ICR SCID outbred mice were obtained from Taconic (Germantown, NY). The mice were housed five animals per cage in sterile micro-isolator cages in a temperature- and humidity-controlled room with a 12-h light/12-h dark schedule. The animals were fed autoclaved rodent chow (Ralston Purina, St. Louis, MO) and water ad libitum. Animals were anesthetized for injections with isoflurane (Baxter Healthcare, Deerfield, IL) at a rate of 2.5% with 0.4 liters of oxygen through a nonrebreathing anesthesia vaporizer. Human prostate PC-3 cells were injected on the bilateral s.c. flank with $\approx 5 \times 10^6$ cells in a suspension of 100 μl of normal sterile saline per injection site. PC-3 cells were allowed to grow 2–3 weeks postinoculation developing tumors ranging in mass from 0.02 to 1.30 g. Mice were administered the radiopharmaceutical and the biodistribution data were determined as described for normal CF-1 mice (see above). Receptor blocking studies (1 h p.i., n = 5) were carried out by administration of 100 μg of commercially available BBN[7-14] 15 min before the administration of the [^{64}Cu-NOTA-8-Aoc-BBN(7-14)NH_2].

MicroPET/CT Imaging and Data Analysis. MicroPET tissue data imaging analysis was accomplished by using a MOSAIC small animal PET unit (Philips, Mahwah, NJ). The unit has a gantry diameter of 21 cm, a transverse field of view (FOV) of 12.8 cm and an axial length of 11.6 cm. The scanner operates in a 3D volume imaging acquisition mode. Small animals were frequently laser-aligned at the center of the scanner FOV for subsequent imaging. A mouse bearing xenografted human PC-3 prostate tumors was administered a 1.5-mCi dose of [^{64}Cu-NOTA-8-Aoc-BBN(7-14)NH_2] in 150 μl of sterile saline via i.v. injection into the tail vein. At 24 h p.i., the mouse was killed by CO_2 administration and placed on its prone position on a custom-built cradle. The cradle was mounted with image fusion makers that served as reference points for succeeding image coregistration of PET/CT. The prostate tumor-bearing

mouse was imaged, and data were collected by using an emission MicroPET scan protocol. MicroPET image reconstruction was performed with a 3D row action maximum likelihood algorithm with out tissue attenuation correction. The MicroPET data were filtered with a 1.1-mm Gaussian FWHM filter.

The MicroCT unit (Siemens, Nashville, TN) consists of a CCD x-ray detector and an 80-kVp microfocus x-ray source (40-μm focal spot). MicroCT imaging was performed immediately after MicroPET imaging for the purpose of anatomic/molecular data fusion. MicroCT imaging was performed and concurrent image reconstruction was achieved with the use of a fanbeam (Feldkamp) filtered back projection algorithm. Coregistration, visualization, and image analysis of PET/CT data were achieved with the Amira 3.1 software package (TGS, Berlin, Germany).

This work was supported with resources and the use of facilities at the Harry S. Truman Memorial Veterans' Hospital and the University of Missouri School of Medicine. It was funded in part by a Department of Veterans' Affairs Merit Award, National Institutes of Health Grants 1 P50 CA103130-01 and DHHS-R01-CA72942 (to T.L.R., G.L.S., and S.D.F.), and a Veterans' Affairs Veterans Integrated Service Network 15 Career Development Award.

1. Kwekkeboom D, Krenning EP, de Jong M (2004) *J Nucl Med* 41:1704–1713.
2. Krenning EP, de Jong M (2000) *Ann Oncol* 11:267–271.
3. Blum JE, Handmaker H (2002) *Curr Pharm Des* 8:1815–1826.
4. Blum J, Handmaker H, Rinne NA (2002) *Curr Pharm Des* 8:1827–1836.
5. Behr TM, Gotthardt M, Barth A, Behe M (2001) *Q J Nucl Med* 45:189–200.
6. Signore A, Annovazzi A, Chianelli M, Corsetti F, Van de Wiele C, Waterhourse R, Scopinaro F (2001) *Eur J Nucl Med* 28:1555–1565.
7. Okarvi SM (2001) *Eur J Nucl Med* 28:929–938.
8. Liu S, Edwards DS (1999) *Chem Rev* 99:2235–2268.
9. Blok D, Feitsma RIJ, Vermeij P, Pauwels EJK (1999) *Eur J Nucl Med* 26:1511–1519.
10. Goodwin DA, Meares CF (1999) *Cancer Biother Radiopharm* 14:145–152.
11. Krenning EP, Kwekkeboom DJ, Bakker WH, Breeman WAP, Kooij PPM, Oei HY, Hagen M, Postema PTE, Jong M, Reubi JC, *et al.* (1993) *Eur J Nucl Med* 20:716–731.
12. Smith CJ, Volkert WA, Hoffman TJ (2005) *Nucl Med Biol* 32:733–740.
13. Smith CJ, Volkert WA, Hoffman TJ (2003) *Nucl Med Biol* 30:861–868.
14. Markwalder R, Reubi JC (1999) *Cancer Res* 59:1152–1159.
15. Pinski J, Halmos G, Yano T, Szepeshazi K, Qin Y, Ertl T, Schally AV (1994) *Int J Cancer* 57:574–580.
16. Sun B, Schally AV, Halmos G (2000) *Regul Pept* 90:77–84.
17. American Cancer Society (2007) *Cancer Facts and Figures* (Am Cancer Soc, Atlanta, GA).
18. Carducci MA, DeWeese TL, Nelson WG, Simons JW, Sinibaldi V, Eisenberger MA (1996) *Semin Oncol* 23:56–62.
19. Newling DW (1997) *Urol Res* 25:S73–S78.
20. Tang DG, Porter AT (1997) *Prostate* 32:284–293.
21. Anderson CJ, Welch MJ (1999) *Chem Rev* 99:2219–2234.
22. Rogers BE, Manna DD, Safavy A (2004) *Cancer Biother Radiopharm* 19:25–34.
23. Rogers BE, Bigott HM, McCarthy DW, Della Manna D, Kim J, Sharp TL, Welch MJ (2003) *Bioconjugate Chem* 14:756–763.
24. Chen X, Park R, Hou Y, Tohme M, Shahinian AH, Bading JR, Conti PS (2004) *J Nucl Med* 45:1390–1397.
25. Yang Y-S, Zhang X, Xiong Z, Chen X (2006) *Nucl Med Biol* 33:371–380.
26. Bass LA, Wang M, Welch MJ, Anderson CJ (2000) *Bioconjugate Chem* 11:527–532.
27. Sprague JE, Peng Y, Sun X, Weisman GR, Wong EH, Achilefu S, Anderson CJ (2004) *Clin Cancer Res* 10:8674–8682.
28. Boswell CA, Sun X, Niu W, Weisman GR, Wong EH, Rheingold AL, Anderson CJ (2004) *J Med Chem* 47:1465–1474.
29. Sun X, Wuest M, Weisman GR, Wong EH, Reed DP, Boswell CA, Motekaitis R, Martell AE, Welch MJ, Anderson CJ (2002) *J Med Chem* 45:469–477.
30. Kukis DL, Li M, Meares CF (1993) *Inorg Chem* 32:3981–3982.
31. Kukis DL, Diril H, Greiner DP, DeNardo SJ, DeNardo GL, Salako QA, Meares CF (1994) *Cancer* 73(Suppl):779–786.
32. Wieghardt K, Bossek U, Chaudhuri P, Herrmann W, Menke BC, Weiss J (1982) *Inorg Chem* 21:4308–4314.
33. Delgado R, Sun Y, Motekaitis RJ, Martell AE (1993) *Inorg Chem* 32:3320–3326.
34. Smith CJ, Gali H, Sieckman GL, Hayes DL, Owen NK, Mazuru DG, Volkert WA, Hoffman TJ (2003) *Nucl Med Biol* 30:101–109.
35. Hoffman TJ, Gali H, Smith CJ, Sieckman GL, Hayes DL, Owen NK, Volkert WA (2003) *J Nucl Med* 44:823–831.
36. Smith CJ, Gali H, Sieckman GL, Higginbotham C, Volkert WA, Hoffman TJ (2003) *Bioconjugate Chem* 14:93–102.
37. Maina TM, Nock BA, Zhang H, Nikolopoulou A, Waser B, Reubi J-C (2005) *J Nucl Med* 46:823–830.
38. Garrison JC, Rold TL, Sieckman GL, Figueroa SD, Volkert WA, Jurisson SS, Hoffman TJ (2007) *J Nucl Med*, in press.
39. Kelloff GJ, Hoffman JM, Johnson B, Scher HI, Siegel BA, Cheng EY, Cheson BD, O'Shaughnessy J, Guyton KZ, Mankoff DA, *et al.* (2005) *Clin Cancer Res* 11:2785–2808.
40. Kumar R, Zhuang H, Alavi A (2004) *Radiol Clin North Am* 42:1141–1153.
41. Hofer C, Laubenbacher C, Block T, Breul J, Hartung R, Schwaiger M (1999) *Eur Urol* 36:31–35.
42. Sung J, Espiritu JI, Segall GM, Terris MK (2003) *BJU Int* 92:24–27.
43. Jana S, Blaufox MD (2006) *Semin Nucl Med* 36:51–72.